10-1-2018

Advanced cotton fibers exhibit efficient photocatalytic self-cleaning and antimicrobial activity

Jared Jaksik
The University of Texas Rio Grande Valley

Phong Tran
The University of Texas Rio Grande Valley

Veronica Galvez
The University of Texas Rio Grande Valley

Isaac Martinez
The University of Texas Rio Grande Valley

Darian Ortiz
The University of Texas Rio Grande Valley

See next page for additional authors

Recommended Citation

Jaksik, Jared, et al. "Advanced cotton fibers exhibit efficient photocatalytic self-cleaning and antimicrobial activity." Journal of Photochemistry and Photobiology A: Chemistry 365 (2018): 77-85. https://doi.org/10.1016/j.jphotochem.2018.07.037

Advanced cotton fibers exhibit efficient photocatalytic self-cleaning and antimicrobial activity

Jared Jaksik[a], Phong Tran[a], Veronica Galvez[a], Issac Martinez[a], Darian Ortiz[a], Andy Ly[a], Monica McEntee[b], Erin M Durke[b], Sayeeda TJ Aishee[a], Margaret Cua[a], Ahmed Touhami[c], H. Justin Moore[a], M. Jasim Uddin[a]*

[a]Department of Chemistry
The University of Texas Rio Grande Valley
1201 W University Dr, Edinburg, TX 78539, United States
[b]US Army Edgewood Chemical Biological Center, Aberdeen MD 21010
[c]Department of Physics, 1 West University Boulevard, Brownsville, TX 78520, United States
Phone: 956-665-7462 Fax: 956-665-5006
*Corresponding Author: Email jasim.uddin@utrgv.edu

KEYWORDS

Fibers, Self-cleaning, Gold nanoparticles, Silver nanoparticles, TiO_2, Anti-microbial

ABSTRACT GRAPHIC

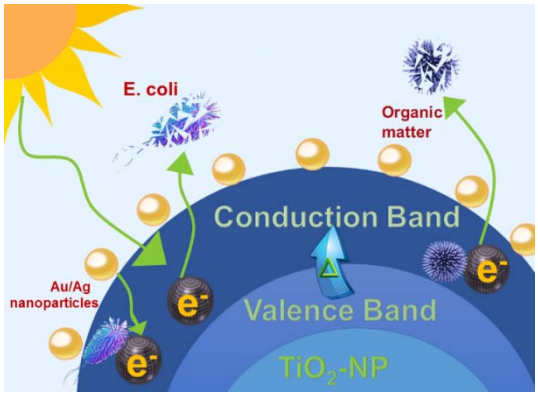

ABSTRACT Functional cotton fibers have a wide range of applications in domestic, commercial, and military settings, and so enhancing the properties of these materials can yield substantial benefits. Herein, we report the creation of functional fibers that are self-cleaning, anti-microbial, and protective against UV radiation. A uniform, and high surface area films of TiO_2 were deposited on cotton fibers and gold / silver nanoparticles were directly incorporated on the nanostructured TiO_2 surface. The synthetic method is simple and the produced TiO_2 film is homogenous and the nanoparticles were shown to be effectively distributed on the surface using a simple photocatalytic reduction method. The Ag/Au-TiO_2 coated fibers was morphologically characterized using atomic force microscopy (AFM) and scanning electron microscopy / energy dispersive X-ray spectroscopy (SEM/EDS), and the self-cleaning properties of noble metal nanoparticle / TiO_2 coated fibers were demonstrated by repeated staining followed by exposure to simulated solar light. The 1 mM Ag-TiO_2 coated fabric was observed to have the largest improvement in rate of stain extinction compared to the untreated fibers with a methylene blue stain, and the 1 mM Au-TiO_2 coated fibers were observed to have the largest improvement versus untreated fibers when stained with Congo red. The fibers maintained consistent photocatalytic activity over multiple cycles, and the resistance of the Ag/Au-TiO_2

coated cotton to degradation was verified using Fourier transform infrared spectroscopy (FTIR). An efficient anti-microbial activity of the fibers was confirmed by exposure of the fibers to bacterial culture (*Escherichia Coli*) and direct observation of antimicrobial activity.

1. INTRODUCTION

The development of advanced fibers has been a popular topic research in the recent past, and fibers with a variety of exceptional properties have been prepared including: hydrophobicity [1], bactericidality [2], UV impermeability [3], and the ability to self-cleanse organic stains [4]. TiO_2 is a well-known photo-catalyst [5] that has been extensively tested and shown to effectively decompose a wide range of organic substances under irradiation with solar light, including methylene blue [6], isothiazolin-3-ones [7], formaldehyde [8], acid orange [9], phenol [10], coffee / wine stains [11], and even the chemical warfare agent Soman [12]. The innate photocatalytic effectiveness of TiO_2 is very high, even under artificial room lighting a layer of TiO_2 possesses sufficient photocatalytic activity to completely mineralize an approximately 1 µm thick hydrocarbon layer every hour [13]. This makes TiO_2 an ideal candidate for a surface photocatalytic coating to produce self-cleaning fibers. Deposition of TiO_2 thin films has been carried out using: (a) surface pre-treatment techniques like RF or MW-plasma activation of the fibers to produce negatively charge functional groups which then adhere the TiO_2 coating [4,14,15], (b) utilization of a TiO_2 emulsion with polymer-generating additives that is sprayed on the fibers and then heated to around 100 °C to generate the TiO_2 containing polymer on the surface [16], and (c) direct growth of TiO_2 on the fibers from a titanium isopropoxide precursor solution [17,18]. The final method of TiO_2 deposition from a titanium isopropoxide based precursor solution via the room temperature sol-gel process was selected for this study as it is well developed / simple to carry out, avoids the use environmentally harmful halogenated organics or other toxic materials, and uses solutions that were observed to be stable for a period of several days which suggests good industrial scalability compared to other methods. This film lends the material enhanced UV protective properties and ensures that the photo-generated excitons only minimally interact with the underlying cellulose fibers, which lends the material enhanced stability over time compared to the TiO_2 nanoparticle-based approaches.

The oxidative photocatalytic action of TiO_2 is due to the generation of oxidizing species at the TiO_2 surface, and the simultaneous reduction of the TiO_2 itself [19]. Reduction of the TiO_2 to Ti_2O_3 or even further to metallic titanium occurs on exposure of TiO_2 to high-energy radiation and produces electron / hole pairs. The reduction of TiO_2 is reversible in the presence of atmospheric oxygen, which allows for the photocatalytic activity of the oxide surface to continue indefinitely [19]. The holes generated from the photoinduced reduction of TiO_2 are trapped at the TiO_2 surface within picoseconds, and the thus trapped holes can survive for microseconds, providing sufficient time for oxidation of surface-adsorbed species to take place [20]. Further if there are any adsorbed hydroxyl-containing species on the oxide surface, hydroxyl radicals can be generated which can go on to oxidize other species [19]. Consideration must also be given to the phase of TiO_2 produced by the synthetic method being used, as the anatase phase has been shown to have superior catalytic activity to either the rutile or brookite phases [19].

Silver nanoparticles have been a topic of extensive research in the recent past because of their antibacterial activity [21]. In addition to possessing antibacterial activity, silver nanoparticles have been shown to reduce the incidence of electron / hole recombination when used in conjunction with TiO_2 [22], which should improve photocatalytic activity. Gold nanoparticles have also been an important topic of research, and have been specifically shown to decrease the bandgap of TiO_2 which improves overall photocatalytic activity [23] and allows for the photocatalytic destruction of certain organic under visible-only / UV filtered lighting conditions where a TiO_2 coating alone is ineffective [12]. In most past studies gold and silver nanoparticles have been prepared as a suspension and then deposited on the surface of interest; while this has advantages for fine tuning the morphology of the nanoparticles [24], it also requires additional preparatory work which makes it less suitable for scalable applications. It was recently discovered that noble metal nanoparticles could be grown directly on the surface of certain polysaccharides, with the native functional groups acting to reduce the $AgNO_3$ (the precursor used to generate silver nanoparticles) or the $AuCl_3$ (the precursor used to generate gold nanoparticles) when exposed to UV radiation [25]. Concerning the synthetic technique and long-term stability of the metallic nanoparticles on the photocatalytic oxide surface, it is well known that silver nitrate and gold chloride, the precursors used in this research, are readily reduced on illuminated oxide surfaces [26].

The aim of this study is to determine if nanostructured gold and silver nanoparticles can be grown directly on the surface of natural cotton fibers that have already been coated with TiO_2 utilizing a sol-gel based method that uniformly coats the fiber material, via direct reduction of $AuCl_3$ / $AgNO_3$ by UV radiation, as well as comparison of the self-cleansing properties of the Ag/Au/TiO_2 coated fabric with differing concentrations of noble metal nanoparticles. Additionally, direct verification of the anti-microbial properties of the Ag/Au-TiO_2 coated fibers is also a priority. For the self-cleansing characterization methylene blue was selected as the primary stain since its degradation pathway is well understood [6], and Congo red was also used to provide secondary verification of the self-cleaning properties. The fiber samples were morphologically characterized using SEM and AFM, the self-cleaning properties analyzed via UV-Vis-DRS, resistance of the fibers to photodegradation determined using FTIR, and distribution of the gold and silver nanoparticles on the surface of the TiO_2 coating verified using EDS.

2. EXPERIMENTAL SECTION

2.1 Preparation and treatment of Au/Ag TiO_2 coated fibers.

Acetone, 2-propanol, titanium isopropoxide, hydrochloric acid, silver nitrate, and glacial acetic acid were purchased from Sigma Aldrich. Gold chloride was purchased from Acros Organics. The raw cotton fibers that were used for morphological characterization were obtained from an agricultural plot in the Rio Grande Valley, Texas. Pure 100% cotton fiber was obtained from Rio Grande Valley, Texas, United States.

The raw cotton fibers were soxhlet extracted with acetone for a period of 3 hours to remove any impurities that may be present like natural fats. After washing, the cotton fibers were allowed to dry at room temperature for twelve hours. The nanostructured interface has been created using the procedure reported elsewhere [17]. The nanosol solution for coating the fibers was prepared as two separate solutions: (a) containing 50 mL of 2-propanol, 1 mL acetic acid, and 5.91 mL titanium isopropoxide and (b) containing 50 mL of 2-propanol, 3 mL concentrated hydrochloric acid, and 0.72 mL of Milli-Q ultrapure water produced from a Milli-Q integral ultrapure water production system. Both solutions were stirred vigorously for a period of 30 minutes, and then solution B was slowly added to solution A under vigorous stirring (400-800 rpm). The cotton fibers were immersed in the thus prepared nanosol solution for 30 seconds, and then allowed to dry for 24 hours at room temperature under normal atmospheric conditions. The nanosol solution was observed to maintain its integrity for one week before precipitating out TiO_2 and becoming qualitatively opaque (the freshly prepared solution is wholly transparent), which suggests that this coating solution is ideal for reuse and cost efficiency over a decent interval of time. Calcination of the fiber to remove any residual solvent was then carried out at 65°C for ten minutes and then 90°C for five minutes under normal atmospheric conditions. The calcined fibers were hydrothermally treated (by boiling in Milli-Q ultrapure water for a period of three hours) to remove excess oxide left behind from the nanosol coating process. The pristine fiber samples were subjected to the same calcination and hydrothermal treatment to ensure that they were a valid control; however, they were not coated with the nanosol TiO_2 solution. For the preparation of the nanoparticle coated fiber samples, 2 mM solutions of gold chloride ($AuCl_3$) and silver nitrate ($AgNO_3$) were prepared and serially diluted to create additional 100 mL solutions of 1 mM and 0.5 mM $AuCl_3$ and $AgNO_3$. Thus a total of six noble metal nanoparticle precursor solutions were prepared. The fiber samples were immersed in these solutions for a period of thirty seconds and then allowed to dry at room temperature under normal atmospheric conditions for 24 hours. Finally, the $AuCl_3$ and $AgNO_3$ / TiO_2 coated fiber samples were exposed to 254 nm UV radiation in an Ultra-Violet Productions CL-1000 ultraviolet crosslinker for a period of thirty minutes. The gold coated samples were seen to take on a purple coloration after the development of the nanoparticles under UV light, while the silver samples took on a characteristic brown color. A total of sixteen fiber samples were prepared, two each of: 0.5 mM Au-TiO_2, 1 mM Au-TiO_2, 2 mM Au-TiO_2, 0.5 mM Ag-TiO_2, 1 mM Ag-TiO_2, 2 mM Ag-TiO_2, TiO_2 only, and pristine cotton. Additional 5 mM Ag-TiO_2 and 5 mM Au-TiO_2 samples were prepared for UV-Vis characterization of the nanoparticles directly. Two replicates of each being prepared for staining with Congo red and methylene blue separately.

Methylene blue (0.001% w/v and 0.1% w/v) and Congo red (0.1% w/v) solutions were prepared from Milli-Q water and the corresponding compounds (purchased from Sigma Aldrich). The fiber samples were scanned via UV-Vis (methodology below) prior to staining, and staining was conducted by simply immersing the fiber samples in a stirred solution of the dye for a period of ten minutes. Stain uptake was qualitatively observed to be less pronounced with the TiO_2 / nanoparticle coated samples compared to the pristine fiber, likely due to the mild hydrophobic properties imparted by the TiO_2 coating, and so the ten-minute interval with stirring was necessary. Staining of the fiber samples was carried out multiple times to verify that the photocatalytic activity of the TiO_2 / nanoparticle coating wasn't decreasing with repeated

staining events followed by UV exposure. The two initial stainings of the methylene blue samples were done with the 0.001% w/v methylene blue solution, while the third staining was done with the 0.1% w/v solution. The Congo red samples were stained only once with the prepared 0.1% w/v Congo red solution. Stain extinction was observed to be virtually complete between staining events. For UV-Vis analysis the fiber samples were mounted on custom made rigid plexiglass sample holders that easily mounted on the UV-Vis and assured that the same area of the fiber samples was being scanned each time. The fiber samples were kept mounted on the sample holders during UV exposure to ensure uniform exposure of the fiber surface.

2.2 Simulated solar light exposure, UV-Vis-DRS, and FTIR characterization.

Exposure of the fiber samples to simulated solar light was carried out using a Honle UV-technology UVACUBE 400 USA under AM 1.5 solar irradiation. Stained fiber samples were placed in the solar simulator and exposed to simulated solar light, and then UV-Vis scans were performed to verify extinction of the stain. UV-Vis measurements were carried out using a Perkin Elmer Lambda 950 UV-Vis-NIR spectrometer equipped with a 150 mm integrating sphere for reflectance measurements. All scans were acquired over the full range of the instrument (2500-250 nm) with 1 nm resolution. Fourier-transform infrared spectroscopic analysis was carried out using a Perkin Elmer Frontier FTIR spectrometer, and data was collected in absorbance mode over the full range of the instrument (4000-450 cm^{-1}). Samples for FTIR analysis were prepared by thoroughly mixing 25 mg of finely divided Au-TiO_2 and pristine cotton fibers with 25 mg of optical grade potassium bromide (purchased from International Crystal Labs), and pressing the mixture into a thin, one-inch diameter pellet using a hydraulic press. The pellets were very fragile and were directly transferred onto copper tape (to act as a rigid backing) with a hole such that the IR beam was obstructed by only the pellet. FTIR samples were repeatedly exposed to simulated solar light in the same Honle solar simulator used for UV-Vis characterization and were scanned at regular two hour intervals.

2.2 Morphologic Characterization

SEM and EDS characterization of the Ag/Au-TiO_2 cotton fiber samples was performed using a JEOL 7800F Field Emission Scanning Electron Microscope, equipped with an Electron Dispersive X-ray Spectroscopy system (EX-37270VUP).

Preparation for AFM characterization of the Ag/Au-TiO_2 cotton fiber samples was carried out by stretching and gluing the cotton fibers to a flat mica surface using double-sided tape. AFM imaging was performed using a Bruker BioScope Catalyst AFM microscope (Bruker, Santa Barbara, CA). Si cantilevers with spring constants of 0.4 N/m and resonance frequencies of 300 kHz were selected for this measurement. AFM height and deflection images were recorded using tapping mode at room temperature. While height images provide quantitative surface topography information, the deflection images exhibit higher contrast of morphological details. Image processing of the data was performed using WSxM 5.0 (Nanotec Electronica, Spain) software.

XRD analysis was carried out using the D2 Phaser 2nd Gen X-ray powder diffractometer D5000 X-ray diffractometer (Bruker).

2.3 Antimicrobial Characterization

Verification of the anti-microbial properties of the Ag/Au-TiO_2 coated cotton fiber was carried out using the Kirby-Bauer disk diffusion method. Agar plates were seeded with *Escherichia coli* bacteria. A 2 cm diameter rough disk, derived from the above prepared fiber samples, was placed in the center of each plate. Plates were then incubated at 37°C for a period of 72 hours, and the zone of inhibition measured in millimeters after incubation.

3. RESULTS AND DISCUSSION

3.1 Morphologic Characterization

The TiO_2 coated cotton fiber samples were analyzed via SEM and the coating was observed to be uniform and thin enough to preserve the definition of the natural surface folds present in the cellulose fiber. This is desirable as these folds increase the exposed surface area of the fiber and can improve photocatalytic efficiency by providing more sites for photoreactions to take place and for the anchoring of nanoparticles. The surface folds are clearly visible before the TiO_2 coating is applied, and the slight reduction in fold definition after the coating is applied is visible (Figure 1-a,b,c,d). The growth of gold and silver nanoparticles on the TiO_2 coated cellulose fibers was verified as successful as a number of small particulates were present (Figure 1-e,f,g,h). Though some loose aggregated nanoparticle clusters are visible in the high magnification images (Figure 1-f,h) they are not grafted to the surface / fiber. Analysis via EDS mapping revealed that the TiO_2 coating was indeed uniform across the entire surface of the fibers with no cracking (Figure 2-a,b,c), which is desirable as it protects the underlying cotton fiber from staining or degradation by acting as a protective barrier. Additionally, spot EDS analysis of the particulates that are clearly visible in Figure 1f indicated that they were silver particles that had been successfully grown on the TiO_2 coated fiber surface.

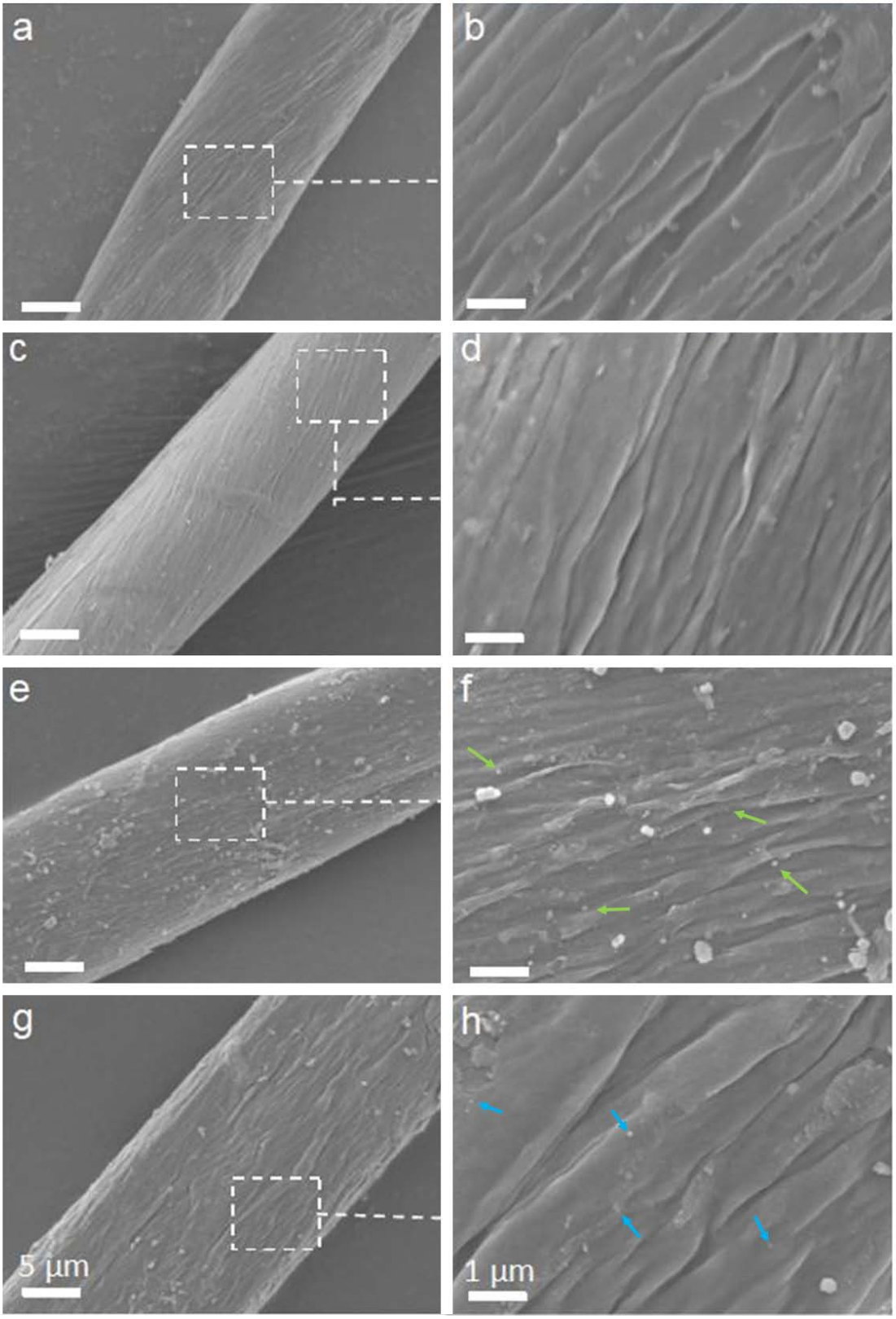

Figure 1: SEM images of TiO_2 coated and pristine cotton fiber at low and high magnification (a,b) Virgin cotton, (c,d) TiO_2 coated cotton fiber, (e,f) Ag-TiO_2 coated cotton fiber with non-

agglomerated Ag nanoparticles marked (green arrows), (g,h) Au-TiO_2 coated cotton fiber with non-agglomerated Au nanoparticles marked (blue arrows). The scales for all images in the same columns are the same.

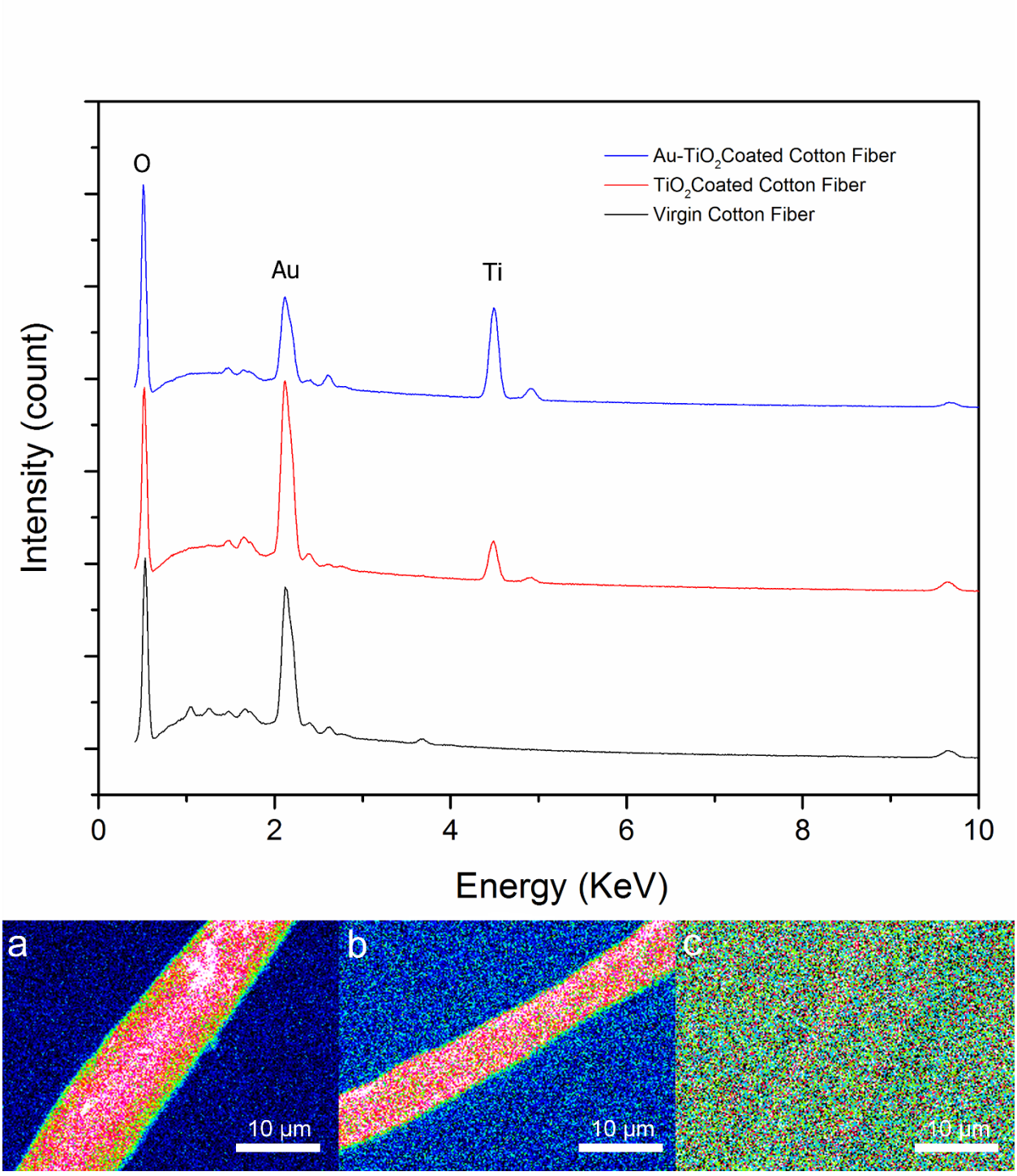

Figure 2. EDS spectra of TiO_2 coated and pristine cotton fiber. Heat map showing distribution of Ti on the surface of the: a) AuTiO_2 coated, b) TiO_2 coated and c) pristine cotton fiber.

AFM analysis of pristine and TiO_2 coated cotton fibers also revealed the TiO_2 coating to be uniformly deposited, with some areas showing TiO_2 aggregation on the surface of the coating (Figure 3). These clusters of TiO_2 increase the available surface area on the surface of the fiber and could contribute to increased photocatalytic activity. From the AFM images it is also apparent that the TiO_2 layer has been evenly adhered to the fiber surface as visibility of the natural folds and creases present in the untreated cotton fiber is noticeably reduced.

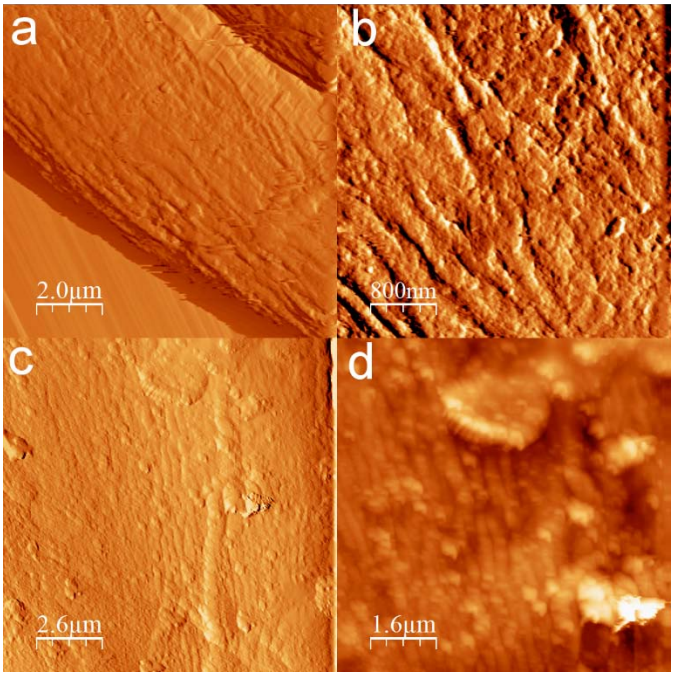

Figure 3. AFM scans of (a,b) pristine cotton fiber and (c,d) TiO_2 coated cotton fiber.

The gold and silver nanoparticle coated fiber samples prepared using 5 mM solutions $AgNO_3$ and $AuCl_3$ were analyzed via UV-Vis after the development of the nanoparticles under UV light (Figure 4). The gold peak at 547 nm matches what would be expected if the gold nanoparticles took on roughly spherical shapes [27], have an average size of 60-80 nm (calculated utilizing available data concerning nanoparticle size and max wavelength of UV-Vis absorption) [28,29], and the width of the peak indicates that nanoparticles constituting a range of sizes were directly generated on the TiO_2 surface coating which is expected given the non size-selective nature of the synthesis method. The silver nanoparticle peak at 440 nm matches what would be expected if the average size of the nanoparticles were between 40 and 50 nm [30]. The intense absorption present in the UV-Vis spectra of all TiO_2 coated samples in the UV region is due to the absorption profile of plain TiO_2. Because the gold and silver nanoparticle peaks occur in the visible region of the spectra it should be noted that the fiber samples took on a characteristic purple (in the case of gold) or brown (in the case of silver) color after deposition of the nanoparticles but prior to staining, which matches the coloration found in the literature when dealing with comparatively large gold and silver nanoparticles [2]. The UV protective properties of the material over untreated cotton are readily apparent as the absorption of all samples but pristine can be seen to dramatically increase in the UV region of the spectra (Figure 4).

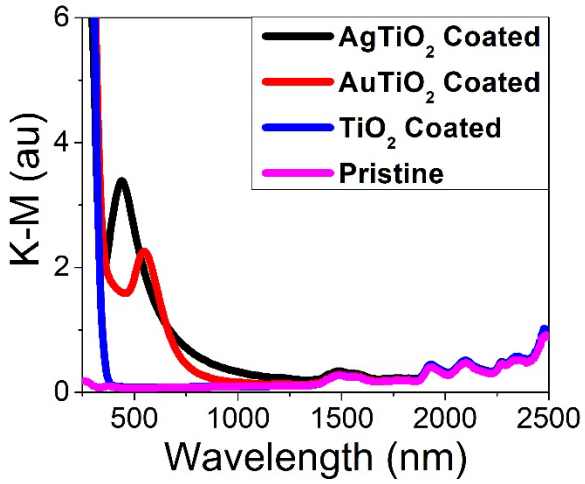

Figure 4. UV-Vis spectra of the fiber samples prior to staining, with the nanoparticle peaks visible.

XRD analysis (Figure 5) of the $AuTiO_2$, $AgTiO_2$, TiO_2, and pristine fiber samples revealed peaks at 16.27˚, 20.67˚, and 22.31˚ which correspond to typical XRD spectra of cotton fibers [31]. Additional peaks were observed at 29.38˚, 43.84˚, and 56.05˚ which are due to the presence of anatase phase TiO_2. The peaks at 20.67˚, and 22.31˚ before and after solar light exposure with stain are indicative of the fiber's polymer skeleton are sustainably stable with the radiation exposure. This structural stability data is in agreement with photocatalytic kinetics and FTIR/chemical stability analysis (Figure 8 and 10).

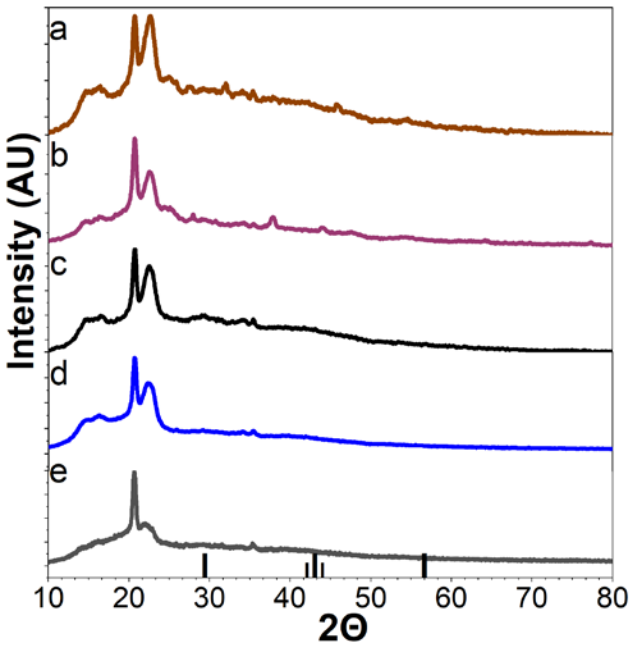

Figure 5. XRD spectra for (a) pre-exposure $AgTiO_2$ coated cotton fibers, (b) pre-exposure $AuTiO_2$ coated cotton fibers, (c) pre-exposure TiO_2 coated cotton fibers, (d) pre-exposure pristine uncoated cotton fibers, and (e) post-exposure TiO_2 coated cotton fibers.

3.2 Photocatalytic Activity

The UV-Vis spectra acquired from the stain extinction testing of the fiber samples clearly show that the methylene blue stain is being destroyed by the titanium oxide / nanoparticle coating at a faster rate than occurs with the pristine cotton sample (Figure 6, S1). The apparent dual peaks are a result of the adsorbed methylene blue being present in monomeric, dimeric, and trimeric forms. Monomeric methylene blue accounts for the smaller peak (apparent as a shoulder of the main peak) around 673 nm, while adsorbed dimeric and trimeric methylene blue have absorption peaks around 596 and 570 nm respectively [32]. The breakdown of the dimeric and trimeric forms can be seen to proceed more rapidly than the decay of the monomeric form. Nonetheless the breakdown of methylene blue proceeds much more rapidly for the fiber samples that have been coated with TiO_2, and further improvement of the rate of decay is obtained when gold or silver nanoparticles are deposited on the fibers (Figure 7, S2). The rate of extinction for each type of sample was obtained by subtracting the pre-stain UV-Vis spectra from the spectra obtained at each time interval and integrating the resulting spectra from 475 to 750 nm. The

extinction of methylene the adsorbed stain can be seen to follow a roughly first order rate of decay (Figure 7), so the rate of decay can be determined via:

$$\ln\left(\frac{[C]}{[C]_0}\right) = -kt$$

and a plot of $\ln([C]/[C]_0)$ is presented below as Figure 7. All of the tested fiber samples had a more rapid rate of stain extinction than the pristine sample, with the 1 mM $AgTiO_2$ sample showing a 200% improved rate of stain extinction compared to the pristine sample. All kinetic constants are presented in the supplemental information for the sake of completion (Figure S3). The R^2 value for the kinetic data (Figure 7) remains in between ~0.85 and 0.97, indicating that the photocatalytic degradation reaction follows roughly first order kinetics. A complicating factor in the evaluation of methylene blue stain extinction is the fact that methylene blue is present as monomeric, dimeric, and trimeric forms, and it appears that the monomer is destroyed more slowly as the rate of stain removal tends to decrease with time, although this effect was not apparent for the pristine sample. This apparent dependence of photocatalytic effectiveness on the oligomerization of methylene blue is expected as the different oligomers are expected to have unique reactivities. Furthermore, it is apparent from the data that deposition of gold nanoparticles has a favorable effect on the rate of extinction of Congo red while only a negligible or non-effect on the rate of extinction of methylene blue. Inversely deposition of silver metal nanoparticles had a favorable effect on the rate of extinction of Methylene blue while only a negligible or non-effect on the rate of extinction of Congo red. The likely reasons for this are discussed below and include the overlap of the absorption spectrum of the dyes with the active absorbance regions of the noble metal nanoparticles.

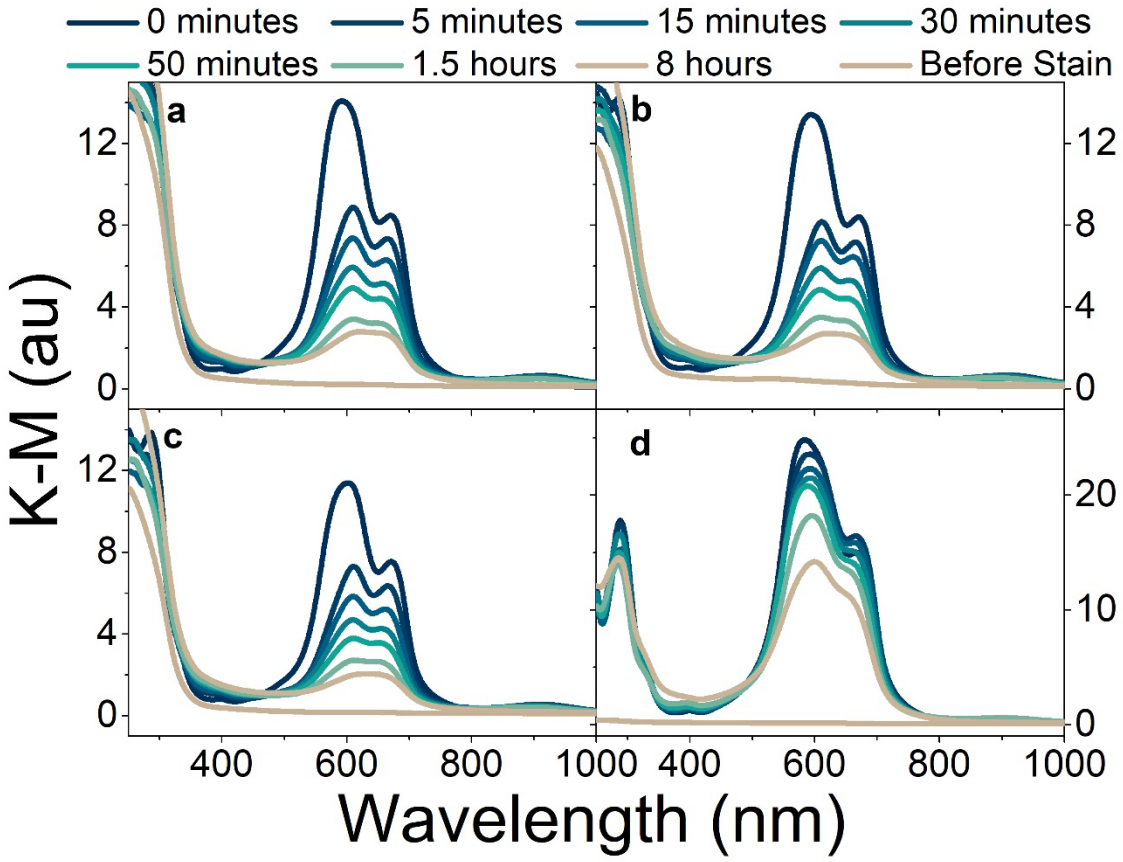

Figure 6: UV-Vis spectra of the TiO_2 / nanoparticle coated samples after staining with methylene blue, and upon exposure to simulated solar light: a) 1 mM $AgTiO_2$ coated fibers, b) 1 mM $AuTiO_2$ coated fibers, c) TiO_2 coated fibers and d) pristine cotton fibers. Note that the rate of stain extinction / fibers self-cleaning is dramatically increased on the nanoparticle-coated samples.

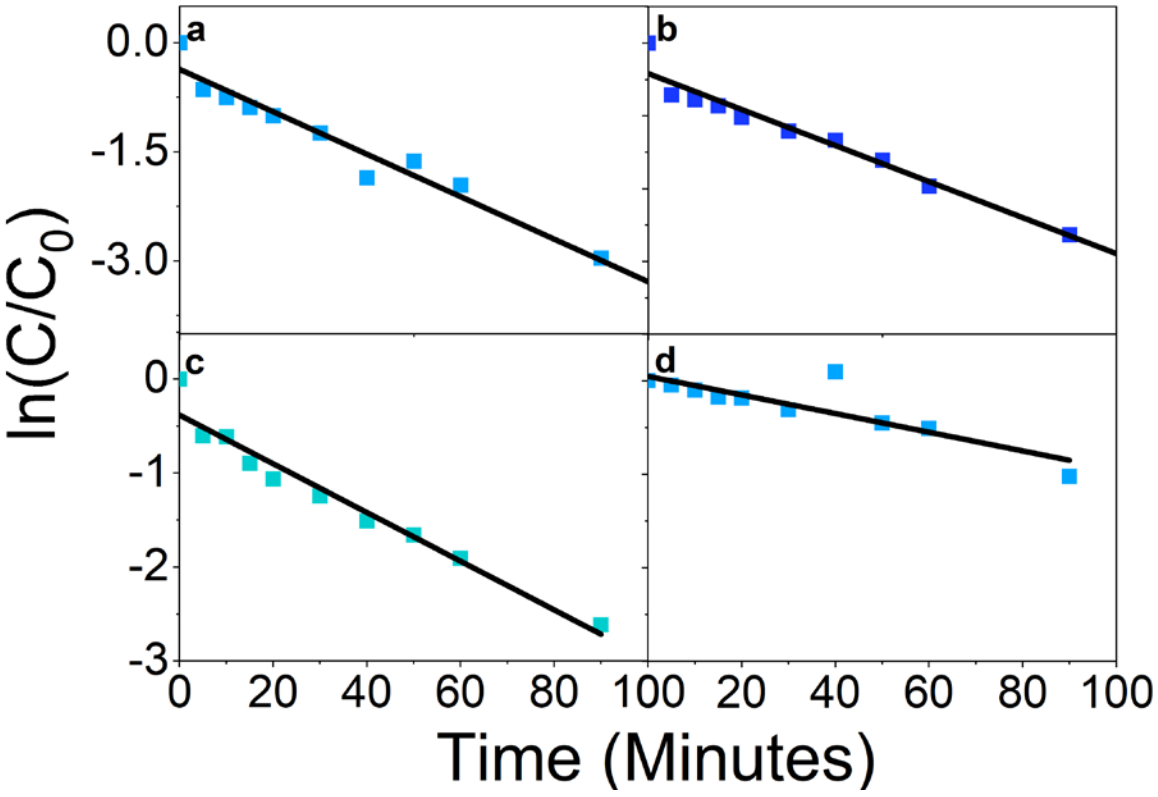

Figure 7. The natural log of the ratio of methylene blue peak area to starting peak area upon repeated exposure to simulated solar light for TiO_2 / nanoparticle coated fiber samples: a) 1 mM $AgTiO_2$ coated fibers, b) 1 mM $AuTiO_2$ coated fibers, c) fibers coated with TiO_2 only and d) pristine cotton fibers. Note that the rate of stain extinction is much slower for the pristine fiber sample.

Verification that the photocatalytic activity of the $Au/AgTiO_2$ coated fibers does not decrease over time is important, and so all fiber samples were subjected to three cycles of staining, followed by exposure to simulated sunlight until the stain was virtually eliminated. The fiber samples displayed remarkable consistency of stain removal over multiple cycles, with the obtained rate constants of stain removal being virtually the same in the case of the 1 mM $AgTiO_2$ coated sample (Figure 8, S8). "Because the kinetic rates of stain degradation do not change over multiple staining cycles, it can be seen that the photocatalytic activity of the produced coating is stable even over a significant length of time (Figure 8, S8). It should be noted that the total time under simulated solar irradiation presented in Figure 8 is ~ 11 hours, and no change in the rate of stain extinction was noted over these three discrete staining events. From our previous report it was seen that decreasing the intensity of the light resulted in a reduced rate of photocatalytic activity [39]. It showed a certain dependency on the applied light dose, which is indicative of TiO_2 would predominantly control these photocatalytic processes and Au/Ag promotes the process efficiency [17,33]. In Figures S9,10, the IR spectra of the cellulose fibers before and

after TiO_2 grafting are compared (curves a ~e). The aim of the experiment was to ascertain whether IR spectroscopy could be informative on the grafting mechanism, which is expected to involve the esterification of OH groups located on the external surface of the fibers (Figure S9) and the fibers stability with light exposure (Figure S10). The spectrum of the virgin sample (Figure 5, Curve 1) is characterized by an intense and broad band in the 3600–3100 cm^{-1} range, associated with inter- and intra-chain OH–O groups (τ) of the interacting chains as reported in Fig. S10a-d. A peak at ~1600 cm^{-1} is also indicative of the presence of interstitial or adsorbed water. The absorptions in the 3000–2800 and 1450–1350 cm^{-1} ranges are due to the ν(CH) and δ(CH) modes. Finally, the complex absorption in 1250–900 cm^{-1} range is mainly associated with stretching mode of C–O–C groups of the fiber framework. All the above-mentioned groups are mainly located inside the films. This is demonstrated by the spectrum of the fibers after grafting (Figure S10, Curve c-d), which is substantially unaltered. It is quite remarkable that being the IR spectrum of the treated sample totally dominated by the spectrum of the fiber, the contribution of the TiO_2 phase which should appear is also negligible. In conclusion, the photostability of the cellulose fibers is illustrated in Figure S10 a-d, where the curves a–d correspond to the sample exposed to solar-like light for 10 hours. It can be seen that the absorption band at ~3400 cm^{-1} and the complex absorption in the range 1650–1050 cm^{-1} characteristic of the fibers are mostly unchanged. These four curves indicate that the chemical structure of cellulose fiber is not substantially altered upon exposure to solar-like light. In our opinion this is due to the homogeneous character of TiO_2 film which completely adheres and protects the fibers from aggression of O_2 and OH species generated during the exposure to the light [16].”

This suggests that the surface coating is not being damaged during the process of stain removal, and the photocatalytic activity of the samples will remain roughly unchanged over multiple staining / stain removal events. It is important to note that the concentration of the stain had no apparent effect on the rate of stain removal, as staining for the first two cycles was performed using a 0.001% w/v methylene blue solution, and staining for the third cycle used a 0.1% w/v solution and no difference in extinction rate was observed. This suggests that the photocatalytic activity of the coating does not decrease with increased stain saturation, at least at practical levels of staining.

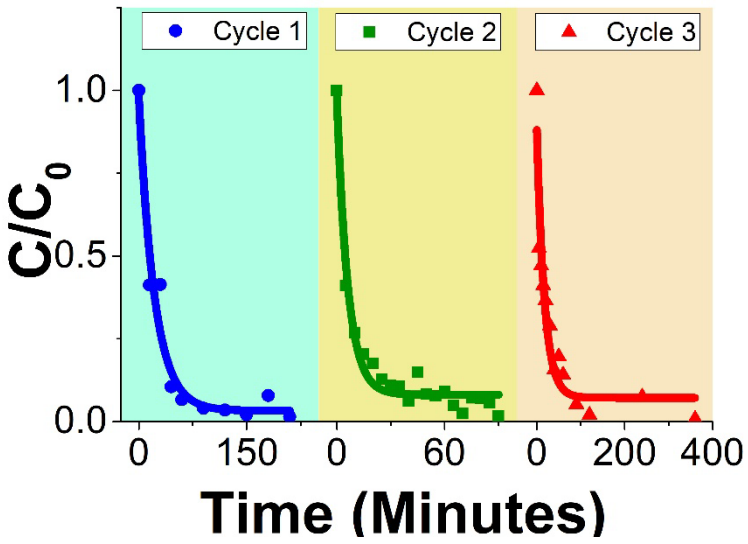

Figure 8. C/C0 data for the 1 mM $AgTiO_2$ sample over repeated cycles of staining and UV exposure. Note how extinction proceeds in the same way each time.

Staining with Congo red was also performed to evaluate the photocatalytic performance with a different, less easily broken-down stain (Figure not shown for the sake of brevity, and Figure S4). In general, the extinction of Congo red can be seen to proceed more slowly than methylene blue, with the rate of extinction of Congo red stained on pristine cotton being roughly half that of methylene blue stained on pristine cotton. The improvement in the rate of stain extinction of the coated samples over the pristine samples was also less pronounced when Congo red was tested, with the 1 mM $AuTiO_2$ sample demonstrating the best performance in this case with a 65% improvement in the rate of stain removal when compared to the pristine fibers (S5,S6). Congo red taking longer to degrade is expected as it has been found to take roughly twice as long as methylene blue to photocatalytically degrade [34], however the decrease in the photocatalytic effect of the Ag/Au TiO_2 coating is notable. This effect can be partially accounted for by the fact that Congo red, while having its main absorption peak at 496 nm, also has two absorption peaks in the UV region at 236 and 338 nm [35]. Because of this, it is likely that some of the incident photocatalytically useful UV and near UV radiation was absorbed by the Congo red stain itself rather than interacting with the $Ag/AuTiO_2$ layer, decreasing the apparent efficiency of the catalytic coating. Compounds such as Congo red which absorb high-energy incident radiation are a good example of why Au / Ag nanoparticle-based photosensitizers are important for photocatalytic applications; by decreasing the bandgap of TiO_2 and increasing the wavelength range in which photons can be harnessed for photocatalysis, compounds which inherently absorb high-energy incident photons can still be degraded. This is likely the reason that the majority of the nanoparticle coated samples displayed better performance than the sample coated with TiO_2 only when stained with Congo red. Additionally, the gold nanoparticle coated samples displayed markedly better photocatalytic activity than the silver coated samples when stained with Congo red (S7), and the reason for this could be explained by the higher wavelength of the gold nanoparticle peak relative to the silver peak, and thus the decreased overlap with the Congo red peaks. This strongly suggests that electron transfer is taking place

between the gold nanoparticles and the TiO_2 coating, and that the gold nanoparticles are acting as photosensitizers. A complicating factor in interpreting the kinetic data directly is the non-first order rate of stain extinction observed for the samples not impregnated with nanoparticles, which was also observed in previous works [23]. This complicates direct comparison of the kinetic constants with one another however qualitatively it can still be seen that the rate of stain extinction is improved for the metallic nanoparticle impregnated samples (Figure 6).

3.3 Fiber Stability

The cotton fibers' stability of photocatalytic activity over time, and confirmation that the cellulose was not being photocatalytically destroyed was provided by FTIR analysis of the Au-TiO_2 coated fibers at regular intervals after UV exposure (Figure 9, Figure S9-S10). Degradation of the fiber would be evidenced by changes in the FTIR spectra corresponding to destruction of the cellulosic backbone, however no changes in the spectra are observed. Characteristic peaks that can be observed include a broad O-H stretching band at 3378 cm^{-1}, the C-H stretching band at 2900 cm^{-1}, and the H-O-H bending band at 1650 cm^{-1} [36], which is observed to be more intense in the Au-TiO_2 coated fiber than in the pristine fiber, however this may also be due to the somewhat hydrophobic nature of the potassium bromide used to prepare the fibers for FTIR analysis. The TiO_2 band is expected to appear at ~700 cm^{-1}, and indeed the Au-TiO_2 absorption spectra lack the "dip" observed in the spectra of pristine cotton near 700 cm^{-1}, which suggests that the TiO_2 while not immediately visible is indeed present as a relatively broad peak [37]. Reduction of the intensity of C-H stretching band at 2900 cm^{-1} was also observed. Overall, the consistency of the FTIR spectra after ten hours of exposure to simulated solar light suggests that the Au-TiO_2 coated fibers possesses long-term photo stability.

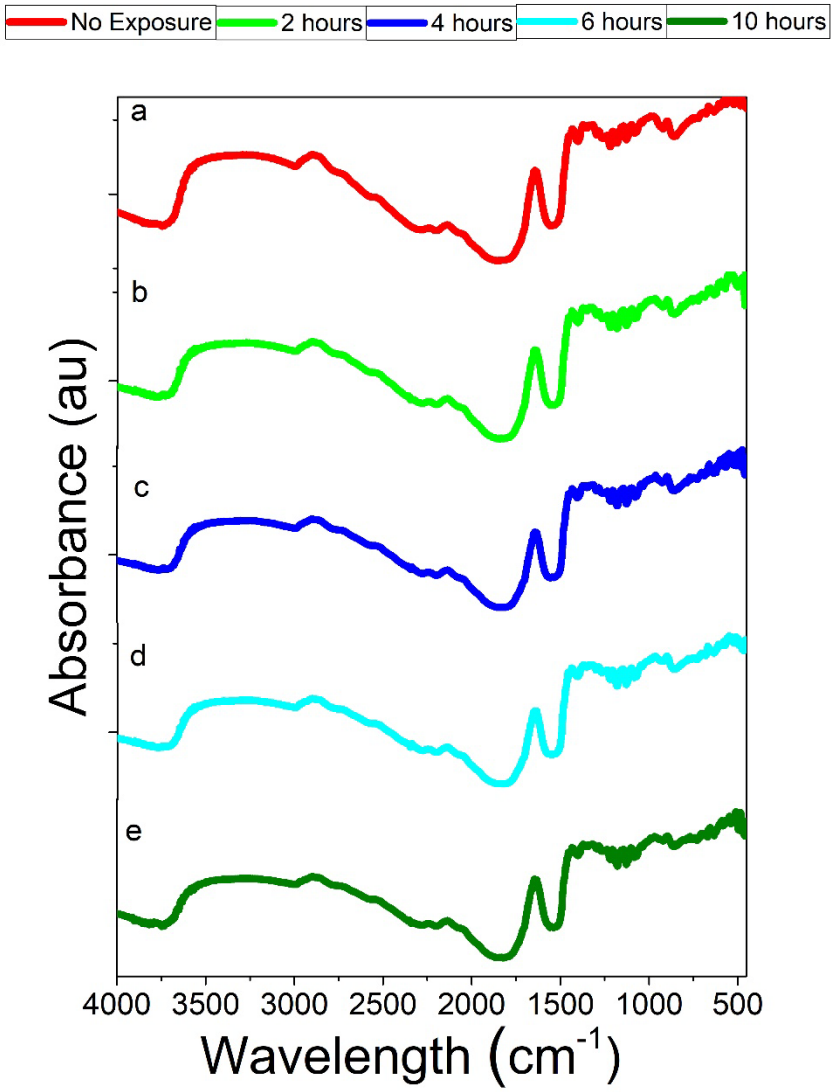

Figure 9. FTIR spectra of the $AuTiO_2$ coated fibers after repeated exposure to simulated solar light for exposure times of (a) no exposure, (b) 2 hours, (c) four hours, (d) six hours and (e) ten hours. The spectra are basically unchanged over time indicating minimal degradation.

3.3 Antimicrobial Activity

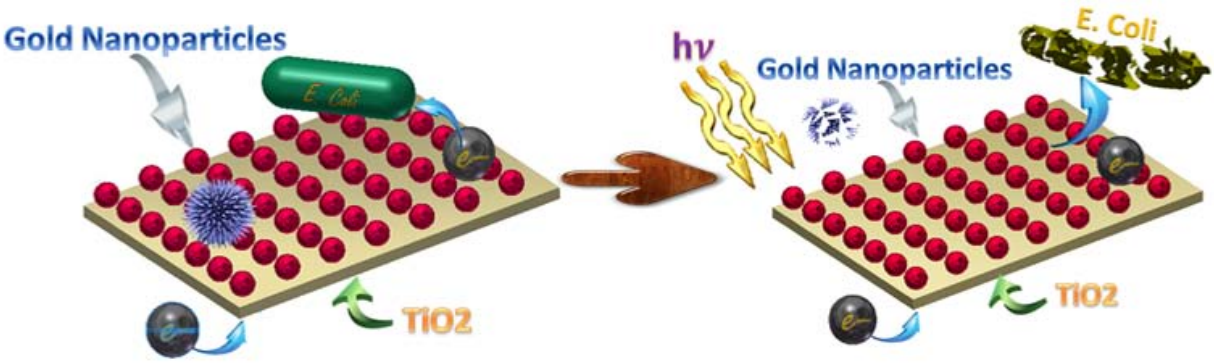

Figure 10. Schematic representation of the antimicrobial activity of the coated fibers: a) before light exposure and b) after light exposure.

The nanoparticle coated fiber samples are expected to show antimicrobial activity in addition to the stain cleansing properties via the mechanism outlined in the abstract graphic and Figure 10. Testing of the anti-microbial properties of the Ag/Au-TiO_2 coated fiber demonstrated that the prepared fiber samples were resistant to gram negative E. Coli microbial contamination as evidenced by the zone of inhibition that was present around the fibers after inoculation and incubation of the plates (Figure 11). It should be noted that the degree of inhibition for the gold and silver nanoparticle coated samples was about equivalent. This result was expected given the widespread study and utilization of silver nanoparticles for their bactericidal properties, and the recent utilization of gold nanoparticles for the same purpose. The TiO_2 and pristine cotton fiber samples exhibited little to no bacterial inhibition, which is notable as some limited degree of bactericidal activity would be expected simply from the reducing / oxidizing potential generated by the TiO_2 layer, and while the oxide alone likely generates some anti-microbial activity, it is apparently much more pronounced with the gold and silver nanoparticle containing samples [19]. It is likely however that bacteria located directly on the illuminated fiber samples coated with TiO_2 only would be quickly removed by the oxidizing power of the TiO_2 and the reactive species generated at the surface, as *E. coli*, *Staphylococcus aureus*, and *Pseudomonas aeruginosa*, the bacteria responsible for common skin infections / MRSA (methicillin-resistant Staphylococcus aureus) and hospital-acquired antibiotic resistant infections respectively, haveeach been experimentally observed to be killed rapidly on illuminated TiO_2 surfaces[38] Furthermore the toxic compounds produced by bacteria can themselves be certainly decomposed by the catalytic action of TiO_2. However, this localized effect is insufficient if the fiber is to be deployed as clothing material, as the entirety of the fiber should be kept free from microbes, not just the outermost exposed surface, thus the relatively large zone of exclusion provided by the incorporation of gold and silver nanoparticles is desirable. One proven mechanism of bactericidal action for both gold and silver nanoparticles includes the disruption of cysteine / disulfide bonds in the proteins on the exterior of bacterial cell walls leading to decreased cell wall integrity, direct inhibition of ATP production, ribosomal activity [39], and DNA degradation [40].

Free radical generation has also been proposed to be an active bactericidal mechanism for silver nanoparticles [41]. The reaction between silver nanoparticles and the membrane structures of both gram positive and gram negative are not fully understood, however the formation of "pits" in the out membranes due to the presence of silver nanoparticles, leading to increased membrane permittivity and ultimately cell death have been observed [41]. However there remains a strong argument for the free radicals generated by silver nanoparticles to be the main causal mechanism behind the antimicrobial effects, as the inclusion of an antioxidant in one study was found to eliminate the anti-microbial action of silver nanoparticles [41]. Furthermore it has been suggested that the evolution of silver ions produced from the silver nanoparticles via their oxidation by the holes produced on the TiO_2 layer may be another mechanism by which the TiO_2 / Ag nanoparticle hybrid surface exhibits antimicrobial activity, as a similar mechanism has been observed with TiO_2 / copper hybrid surfaces [42]. Our results suggest that some combination of the above outlined plays an active role in improving the antimicrobial activity of the nanoparticle coated fiber samples, and further elucidation of the mechanism behind the observed antimicrobial properties could be had testing the nanoparticle coated fibers in the presence of an antioxidant. The gold and silver nanoparticle coated fibers showed similar antibacterial activity, and fine tuning of the nanoparticle surface chemistry could potentially even further improve the anti-bacterial properties of the Au-TiO_2 coated fiber and lend it increased antibacterial activity against particularly hazardous bacteria [43]. Figure 10 demonstrates the mechanism behind the most active bactericidal pathway in this photocatalytically active material, namely, the generation of electrons and holes that react through the mechanisms outlined above to destroy bacteria in proximity to the photocatalytically active nanostructured surface.

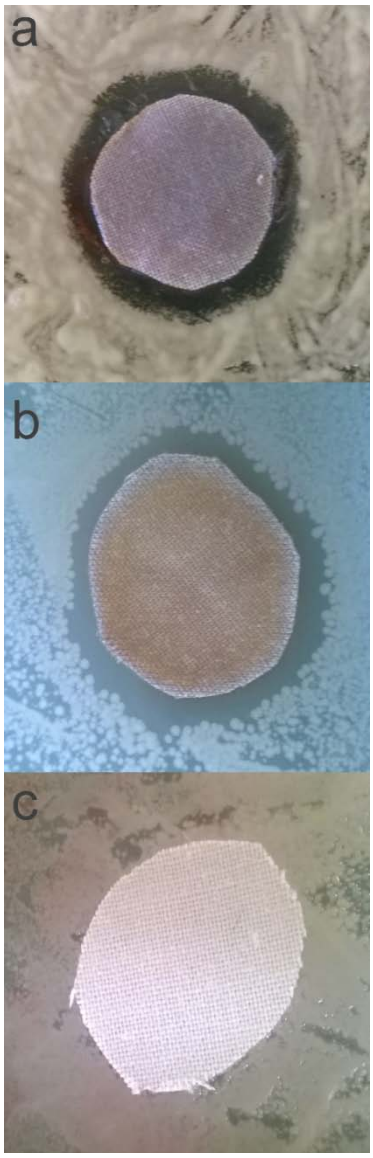

Figure 11. Results of the Kirby-Bauer disk diffusion test with the exclusion zones around the fiber samples clearly visible for: (a) Au-TiO_2 coated cotton fibers, (b) Ag-TiO_2 coated cotton fibers, and (c) pristine cotton fibers.

4. Conclusion

The TiO_2 coating was successfully deposited on cotton fiber and was confirmed by SEM to be both thin and homogenous, which indicates that the simple sol-gel deposition process is well-suited for coating cellulose fibers. Gold and silver nanoparticles were directly grown on the surface and the photocatalytic activity of this nanoparticle / TiO_2 coated fibers was confirmed. Variance in photocatalytic activity between Au and Ag nanoparticle incorporated TiO_2 coated samples confirms that the nanoparticles are having a photosensitizing effect, and their performance with respect to the untreated / only TiO_2 treated fibers indicated that Ag/Au nanoparticles are able to significantly improve the photocatalytic properties of the TiO_2 coating. Consistency of the FTIR spectra after exposure to simulated solar light, as well as the similar

rates of photocatalysis over multiple cycles confirm that photodegradation of the fibers / coating does not take place when exposed to solar light and suggests that these fibers would be suitable for long-term deployment in domestic or commercial applications. Furthermore, the Ag/Au-TiO_2 coated fabric was also confirmed to have marked antimicrobial activity, which further expands the potential applications of fibers coated with TiO_2 and gold / silver nanoparticles.

Acknowledgements:

Jared Jaksik gratefully acknowledges the MSRDC and Department of Defense for his graduate research fellowship thru Award # D01_W911SR-14-2-0001-0003. This research work was partially supported by Welch Foundation Departmental Grant BX-0048. Dr. Karen Martirosyan is gratefully acknowledged for making the FESEM available during the experiments.

References:

[1] H. Tokuhisa, S. Tsukamoto, S. Morita, S. Ise, M. Tomita, N. Shirakawa, Fabrication of micro-textured surfaces for a high hydrophobicity by evaporative patterning using screen mesh templates, Appl. Surf. Sci. 400 (2017) 64–70. doi:10.1016/j.apsusc.2016.11.213.

[2] Z. Li, J. Meng, W. Wang, Z. Wang, M. Li, T. Chen, C.-J. Liu, The room temperature electron reduction for the preparation of silver nanoparticles on cotton with high antimicrobial activity, Carbohydrate Polymers. 161 (2017) 270–276. doi:10.1016/j.carbpol.2017.01.020.

[3] M.R. Nateghi, M. Shateri-Khalilabad, Silver nanowire-functionalized cotton fabric, Carbohydrate Polymers. 117 (2015) 160–168. doi:10.1016/j.carbpol.2014.09.057.

[4] T. Yuranova, D. Laub, J. Kiwi, Synthesis, activity and characterization of textiles showing self-cleaning activity under daylight irradiation, Catalysis Today. 122 (2007) 109–117. doi:10.1016/j.cattod.2007.01.040.

[5] A. Fujishima, K. Honda, Electrochemical Photolysis of Water at a Semiconductor Electrode, Nature. 238 (1972) 37–38. doi:10.1038/238037a0.

[6] A. Houas, H. Lachheb, M. Ksibi, E. Elaloui, C. Guillard, J.-M. Herrmann, Photocatalytic degradation pathway of methylene blue in water, Applied Catalysis B: Environmental. 31 (2001) 145–157. doi:10.1016/S0926-3373(00)00276-9.

[7] V. Kandavelu, H. Kastien, K.R. Thampi, Photocatalytic degradation of isothiazolin-3-ones in water and emulsion paints containing nanocrystalline TiO2 and ZnO catalysts, Applied Catalysis B: Environmental. 48 (2004) 101–111. doi:10.1016/j.apcatb.2003.09.022.

[8] C.H. Ao, S.C. Lee, J.Z. Yu, J.H. Xu, Photodegradation of formaldehyde by photocatalyst TiO2: effects on the presences of NO, SO2 and VOCs, Applied Catalysis B: Environmental. 54 (2004) 41–50. doi:10.1016/j.apcatb.2004.06.004.

[9] M. Stylidi, D.I. Kondarides, X.E. Verykios, Visible light-induced photocatalytic degradation of Acid Orange 7 in aqueous TiO2 suspensions, Applied Catalysis B: Environmental. 47 (2004) 189–201. doi:10.1016/j.apcatb.2003.09.014.

[10] M. Alvaro, C. Aprile, M. Benitez, E. Carbonell, H. García, Photocatalytic Activity of Structured Mesoporous TiO2 Materials, J. Phys. Chem. B. 110 (2006) 6661–6665. doi:10.1021/jp0573240.

[11] B. A, Y. T, K. J, Self-cleaning of wool-polyamide and polyester textiles by TiO2-rutile modification under daylight irradiation at ambient temperature, J Photochem Photobiol A Chem. 172 (20050515) 27–34.
[12] M. Alvaro, B. Cojocaru, A.A. Ismail, N. Petrea, B. Ferrer, F.A. Harraz, V.I. Parvulescu, H. Garcia, Visible-light photocatalytic activity of gold nanoparticles supported on template-synthesized mesoporous titania for the decontamination of the chemical warfare agent Soman, Applied Catalysis B: Environmental. 99 (2010) 191–197. doi:10.1016/j.apcatb.2010.06.019.
[13] A. Fujishima, T.N. Rao, D.A. Tryk, Titanium dioxide photocatalysis, Journal of Photochemistry and Photobiology C: Photochemistry Reviews. 1 (2000) 1–21. doi:10.1016/S1389-5567(00)00002-2.
[14] T. Yuranova, A.G. Rincon, A. Bozzi, S. Parra, C. Pulgarin, P. Albers, J. Kiwi, Antibacterial textiles prepared by RF-plasma and vacuum-UV mediated deposition of silver, Journal of Photochemistry and Photobiology A: Chemistry. 161 (2003) 27–34. doi:10.1016/S1010-6030(03)00204-1.
[15] A. Bozzi, T. Yuranova, I. Guasaquillo, D. Laub, J. Kiwi, Self-cleaning of modified cotton textiles by TiO2 at low temperatures under daylight irradiation, Journal of Photochemistry and Photobiology A: Chemistry. 174 (2005) 156–164. doi:10.1016/j.jphotochem.2005.03.019.
[16] N. Veronovski, M. Sfiligoj-Smole, J.L. Viota, Characterization of TiO2/TiO2—SiO2 Coated Cellulose Textiles, Textile Research Journal. 80 (2010) 55–62. doi:10.1177/0040517509104012.
[17] M.J. Uddin, F. Cesano, F. Bonino, S. Bordiga, G. Spoto, D. Scarano, A. Zecchina, Photoactive TiO2 films on cellulose fibres: synthesis and characterization, Journal of Photochemistry and Photobiology A: Chemistry. 189 (2007) 286–294. doi:10.1016/j.jphotochem.2007.02.015.
[18] M.S.A. Amin, M.J. Uddin, M.A. Islam, Removal of azo dye by synthesized TiO2 nanoparticles, Nanomaterials and the Environment. 1 (2012) 18–22. doi:10.2478/nanome-2012-0003.
[19] A. Fujishima, X. Zhang, D.A. Tryk, TiO2 photocatalysis and related surface phenomena, Surface Science Reports. 63 (2008) 515–582. doi:10.1016/j.surfrep.2008.10.001.
[20] Y. Tamaki, A. Furube, M. Murai, K. Hara, R. Katoh, M. Tachiya, Dynamics of efficient electron–hole separation in TiO2 nanoparticles revealed by femtosecond transient absorption spectroscopy under the weak-excitation condition, Phys. Chem. Chem. Phys. 9 (2007) 1453–1460. doi:10.1039/B617552J.
[21] P.L. Taylor, A.L. Ussher, R.E. Burrell, Impact of heat on nanocrystalline silver dressings: Part I: Chemical and biological properties, Biomaterials. 26 (2005) 7221–7229. doi:10.1016/j.biomaterials.2005.05.040.
[22] 2 WANG Hui-Lei1, Preparation of Silver Nanoparticle Loaded Mesoporous TiO_2 and Its Photocatalytic Property, Journal of Inorganic Materials. (2016). doi:10.15541/jim20150535.
[23] M.J. Uddin, F. Cesano, D. Scarano, F. Bonino, G. Agostini, G. Spoto, S. Bordiga, A. Zecchina, Cotton textile fibres coated by Au/TiO2 films: Synthesis, characterization and self cleaning

properties, Journal of Photochemistry and Photobiology A: Chemistry. 199 (2008) 64–72. doi:10.1016/j.jphotochem.2008.05.004.
[24] P. Priecel, H. Adekunle Salami, R.H. Padilla, Z. Zhong, J.A. Lopez-Sanchez, Anisotropic gold nanoparticles: Preparation and applications in catalysis, Chinese Journal of Catalysis. 37 (2016) 1619–1650. doi:10.1016/S1872-2067(16)62475-0.
[25] S. Boufi, A.M. Ferraria, A.M.B. do Rego, N. Battaglini, F. Herbst, M.R. Vilar, Surface functionalisation of cellulose with noble metals nanoparticles through a selective nucleation, Carbohydrate Polymers. 86 (2011) 1586–1594. doi:10.1016/j.carbpol.2011.06.067.
[26] C. Renz, Über die Einwirkung von Oxyden auf Silbernitrat und Goldchlorid im Licht, HCA. 15 (1932) 1077–1084. doi:10.1002/hlca.193201501118.
[27] S. Eustis, M.A. El-Sayed, Why gold nanoparticles are more precious than pretty gold: Noble metal surface plasmon resonance and its enhancement of the radiative and nonradiative properties of nanocrystals of different shapes, Chem. Soc. Rev. 35 (2006) 209–217. doi:10.1039/B514191E.
[28] W. Haiss, N.T.K. Thanh, J. Aveyard, D.G. Fernig, Determination of Size and Concentration of Gold Nanoparticles from UV−Vis Spectra, Anal. Chem. 79 (2007) 4215–4221. doi:10.1021/ac0702084.
[29] Gold Nanoparticles: Properties and Applications, Sigma-Aldrich. (n.d.). http://www.sigmaaldrich.com/technical-documents/articles/materials-science/nanomaterials/gold-nanoparticles.html (accessed April 20, 2017).
[30] Silver Nanoparticles: Properties and Applications, Sigma-Aldrich. (n.d.). http://www.sigmaaldrich.com/materials-science/nanomaterials/silver-nanoparticles.html (accessed April 12, 2017).
[31] M.A. Moharram, T.Z. Abou El Nasr, N.A. Hakeem, X-Ray diffraction and infrared studies on the effect of thermal treatments on cotton celluloses I and II, J. Polym. Sci. B Polym. Lett. Ed. 19 (1981) 183–187. doi:10.1002/pol.1981.130190405.
[32] J. Cenens, R.A. Schoonheydt, Visible spectroscopy of methylene blue on hectorite, laponite B, and barasym in aqueous suspension, Clays and Clay Minerals. 36 (1988) 214–224.
[33] P.T. Hoang, S.T.J. Aishee, G. Grissom, A. Touhami, H.J. Moore, M.J. Uddin, Synthesis of low energy sensitive hybrid photovoltaic cells using carbon nanotubes: A 3D application device, MRS Advances. 2 (2017) 791–798. doi:10.1557/adv.2017.151.
[34] H. Lachheb, E. Puzenat, A. Houas, M. Ksibi, E. Elaloui, C. Guillard, J.-M. Herrmann, Photocatalytic degradation of various types of dyes (Alizarin S, Crocein Orange G, Methyl Red, Congo Red, Methylene Blue) in water by UV-irradiated titania, Applied Catalysis B: Environmental. 39 (2002) 75–90. doi:10.1016/S0926-3373(02)00078-4.
[35] H. Zhu, R. Jiang, L. Xiao, Y. Chang, Y. Guan, X. Li, G. Zeng, Photocatalytic decolorization and degradation of Congo Red on innovative crosslinked chitosan/nano-CdS composite catalyst under visible light irradiation, J. Hazard. Mater. 169 (2009) 933–940. doi:10.1016/j.jhazmat.2009.04.037.
[36] C. Chung, M. Lee, E.K. Choe, Characterization of cotton fabric scouring by FT-IR ATR spectroscopy, Carbohydrate Polymers. 58 (2004) 417–420. doi:10.1016/j.carbpol.2004.08.005.

[37] R. Beranek, H. Kisch, Tuning the optical and photoelectrochemical properties of surface-modified TiO2, Photochem. Photobiol. Sci. 7 (2008) 40–48. doi:10.1039/b711658f.
[38] Visible 405 nm SLD light photo-destroys methicillin-resistant Staphylococcus aureus (MRSA) in vitro. - PubMed - NCBI, (n.d.). https://www.ncbi.nlm.nih.gov/pubmed/19065556 (accessed June 7, 2018).
[39] E. Pizzo, A. Di Maro, A new age for biomedical applications of Ribosome Inactivating Proteins (RIPs): from bioconjugate to nanoconstructs, J Biomed Sci. 23 (2016). doi:10.1186/s12929-016-0272-1.
[40] Y. Cui, Y. Zhao, Y. Tian, W. Zhang, X. Lü, X. Jiang, The molecular mechanism of action of bactericidal gold nanoparticles on Escherichia coli, Biomaterials. 33 (2012) 2327–2333. doi:10.1016/j.biomaterials.2011.11.057.
[41] J.S. Kim, E. Kuk, K.N. Yu, J.-H. Kim, S.J. Park, H.J. Lee, S.H. Kim, Y.K. Park, Y.H. Park, C.-Y. Hwang, Y.-K. Kim, Y.-S. Lee, D.H. Jeong, M.-H. Cho, Antimicrobial effects of silver nanoparticles, Nanomedicine: Nanotechnology, Biology and Medicine. 3 (2007) 95–101. doi:10.1016/j.nano.2006.12.001.
[42] K. Sunada, T. Watanabe, K. Hashimoto, Bactericidal Activity of Copper-Deposited TiO2 Thin Film under Weak UV Light Illumination, Environ. Sci. Technol. 37 (2003) 4785–4789. doi:10.1021/es034106g.
[43] X. Li, S.M. Robinson, A. Gupta, K. Saha, Z. Jiang, D.F. Moyano, A. Sahar, M.A. Riley, V.M. Rotello, Functional Gold Nanoparticles as Potent Antimicrobial Agents against Multi-Drug-Resistant Bacteria, ACS Nano. 8 (2014) 10682–10686. doi:10.1021/nn5042625.